

A NOVEL IMAGE SEGMENTATION TECHNIQUE FOR DETECTION OF BREAST CANCER

L.S.S.Reddy¹, Ramaswamy Reddy², CH.Madhu³ & C. Nagaraju⁴

Breast cancer is currently one of the leading causes of death among women worldwide. This paper presents an approach for detecting in digital mammograms not only the detection and early stage of tumors can also detectable. In difficulty of image segmentation found misclassified pixels leads to ambiguity at correct detection of boundary. The effective classification is possible by NN Classifier. And provide effective Boundary error removing by an N-ary morphological operator. The overall effect of proposed operator resembles N-ary morphological erosion followed by N-ary morphological dilation i.e. we found exact spreading of Cancer Tumor and remove the boundary errors around it.

Keywords: Mammograms, Tumors, Boundary, Erosion, Dilation, Morphology.

1. INTRODUCTION

In detections of cancer tumors have verity of segmentation problems, Filters are used to removing noise and generate effective features for segmenting an image into different classes of interest. These filter outputs are then processed by a classifier to form a segmented image. After forming the segmented image, narrow regions near the boundary between two different classes are occasionally misclassified as a third class. This third "false class" typically appears as narrow areas of misclassified pixels at the boundary. These narrow misclassified regions can occur when the trajectory of the feature vector makes a transition through feature space at the boundary. As the feature vector changes, it can pass through intermediate feature-space regions assigned to a third class unrelated to the two original classes forming the boundary. Such misclassified regions incidentally appear to be present in the results of prior investigators including NIJMN fig[5] to fig[7]. An Neural network classifier and a two-step hybrid "N-ary" post processing operation is proposed to remove these narrow misclassified regions. In the first step, pixels in regions whose neighborhood consists entirely of one texture class are left unchanged; otherwise, the pixel value is set to zero to indicate it is no longer assigned to any class. The neighborhood size is chosen to be proportional to spatial extent of filter channel response. This first step resembles a morphological erosion operation. In the second step, the classified regions are propagated back into the unassigned regions based on the most common class within 8- neighborhoods. This second step resembles a

morphological dilation operation. The combined effect of these two steps is effective in removing the narrow misclassified strips at boundaries between regions.

2. EXISTING METHODS

To detect the boundary of cancer tumors in a digital mammograms the edge based segmentation techniques are first and second order provides an effective segmentation to detect the boundary profiles. Edge detecting an image significantly reduces the amount of data and filters out useless information, while preserving the important structural properties in an image. Edge detectors are a collection of very important local image pre-processing methods.

Sobel Operator: The Sobel operator performs a 2-D spatial gradient measurement on an image. Typically it is used to find the approximate absolute gradient magnitude at each point in an input grayscale image. The Sobel edge detector uses a pair of 3x3 convolution masks, one estimating the gradient in the x-direction (columns) and y-direction (rows). A convolution mask is usually much smaller than the actual image. As a result, the mask is slid over the image, manipulating a square of pixels at a time. The actual Sobel masks are shown below

$$G_x = \begin{bmatrix} -1 & 0 & +1 \\ -2 & 0 & +2 \\ -1 & 0 & +1 \end{bmatrix} \quad G_y = \begin{bmatrix} +1 & +2 & +1 \\ 0 & 0 & 0 \\ -1 & -2 & -1 \end{bmatrix}$$

Prewitt Operator: The Prewitt edge detector is a also much better operator. This operator having a 3x3 masks deals better with the effect of noise. The Prewitt edge detection masks, shown below, are one of the oldest and best understood methods of detecting edges in images. Basically, there are two masks, one for detecting image

¹Director, LBRCE, Mylavaram, A.P., India.

²Associate Prof., Dept. of IT, LBRCE, Mylavaram, A.P., India.

³Asst Prof., Dept. of IT, LBRCE, Mylavaram, A.P., India.

⁴Professor, Dept. of IT, LBRCE, Mylavaram, A.P., India.

²ramaswamyreddya@yahoo.com, ³chmadhu1984@yahoo.co.in,

⁴cncrcse@yahoo.com,

derivatives in X and one for detecting image derivatives in Y. This Prewitt operator is obtained by setting $c = 1$.

$$G_x = \begin{bmatrix} -1 & 0 & 1 \\ -1 & 0 & 1 \\ -1 & 0 & 1 \end{bmatrix} \quad G_y = \begin{bmatrix} 1 & 1 & 1 \\ 0 & 0 & 0 \\ -1 & -1 & -1 \end{bmatrix}$$

Robert Operator: The Robinson edge detector is similar to the Sobel edge detector. The Robinsons row, column and corner masks are shown below

$$G_1 = \begin{bmatrix} 0 & -1 \\ 1 & 0 \end{bmatrix} \quad G_2 = \begin{bmatrix} -1 & 0 \\ 0 & 1 \end{bmatrix}$$

It is symmetrical by the axis. The maximum value is found in the edge magnitude and the edge direction is defined by the maximum value found by the edge magnitude.

Limitations for Existing Methods: Edge-based methods center around contour detection: their weakness in connecting together broken contour lines make them, too, prone to failure in the presence of blurring. The main disadvantage of these edge detectors is their dependence on the size of objects and sensitivity to noise. Further, since conventional boundary finding relies on changes in the grey level, rather than their actual values, it is less sensitive to changes in the grey scale distributions over images as against region based segmentation.

3. PROPOSED METHOD

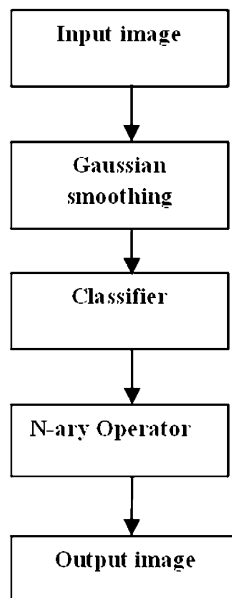


Fig.5: Block Diagram Representation of Proposed Method

The digitized mammogram is filtered by Gaussian Low pass filter. At this stage the noise is removed, and it is introduced due to image acquire and image transmission. Then the filtered images classify the image by using neural network. The classification of the detected NN micro-calcification into benign (non-cancerous lesion) and malignant (cancerous lesions) is performed using a radial basis function network that has a single hidden layer structure. The output of the radial basis function network is 0 for benign and 1 for malignant. After the classification, we get the segmented image. Now to eliminating the narrow misclassified regions proceeds in two steps, beginning with a previously classified image $c(x,y)$, where $c(x,y) \in \{1, 2, 3, \dots, N\}$ and N is the number of classes. In the first step, boundary regions are reset to an unclassified state. In the second step, classes are propagated back into the unclassified regions. Details are given below. In the first step, pixels in the classified image $c(x, y)$ whose neighborhood consists entirely of one class are left unchanged; otherwise, the pixel value is set to zero to indicate that the pixel is no longer assigned to any class. The declassification of these pixels creates a new image

$$I_{s,0}(x, y) = \begin{cases} c(x, y), & \text{if } c(x, y) = c(a, b) \forall (a, b) \in B \\ 0, & \text{otherwise} \end{cases}$$

Where B is a local neighborhood typically it is chosen in some proportion to the spatial extent of the filter channel impulse responses. In the second step, classified regions are propagated back iteratively into the unassigned regions. Each unassigned pixel is assigned to the most prevalent class within the 8-neighborhood surrounding the pixel.

$$i_{s,n+1}(x, y) = \begin{cases} i_{s,n}(x, y), & (x, y) \neq 0 \\ 0, & \text{if all N8 neighbors} = 0 \\ I_{\max}, & \text{otherwise} \end{cases}$$

Where I_{\max} is the nonzero pixel value that occurs the greatest number of times in the 8-neighborhood, $i_{s,n}(x,y)$ is the image at iteration n . In the event of a tie in determining I_{\max} , the pixel is arbitrarily assigned to one of the prevalent classes (other schemes are possible). Step 2 is repeated until all pixels are non-zero, giving the final segmented image $i_s(x, y)$. This propagation affects only unassigned pixels and ceases when all unassigned pixels have been assigned to one of the N classes.

4. RESULTS

The proposed method has also been tested on a wide range of natural and synthetic 512×512 pixel 8-bit grayscale images. In these images, the average gray scale was equalized to prevent biased segmentation results due to leakage of the DC component through the filters [4]-[6]. The results in Fig. 5 illustrate the effects of the proposed method on misclassifications at texture boundaries. The image in Fig. 5(a) consists of an outermost region of

Gaussian-distributed low pass noise, a middle ring of “French canvas”, and an innermost square region of “straw matting” from the NIJMAN database Fig. 5(b) is the classifier output $c(x, y)$ without the proposed method. A prominent band of misclassified pixels is seen along the entire boundary between the outermost texture (noise) and the middle ring of texture (French canvas). Applying the proposed operator to Fig. 5(b) results in the final segmented image $iS(x, y)$ in Fig. 5(c). Comparing Fig. 5(b) and (c), the pixels misclassified as a third texture at the texture boundary are removed by the proposed methods.

Results of Existing Methods

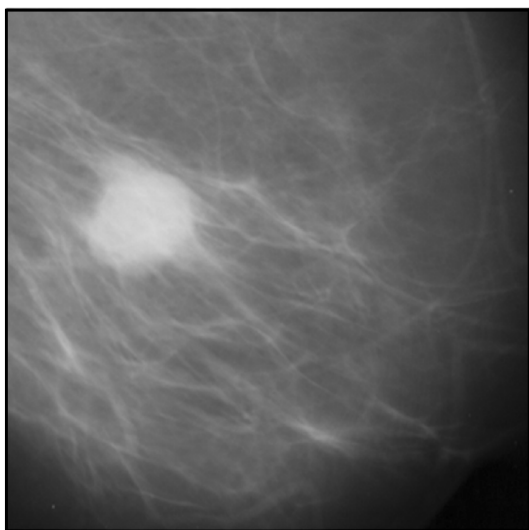


Fig. 1: 512× 512 Original Mammogram

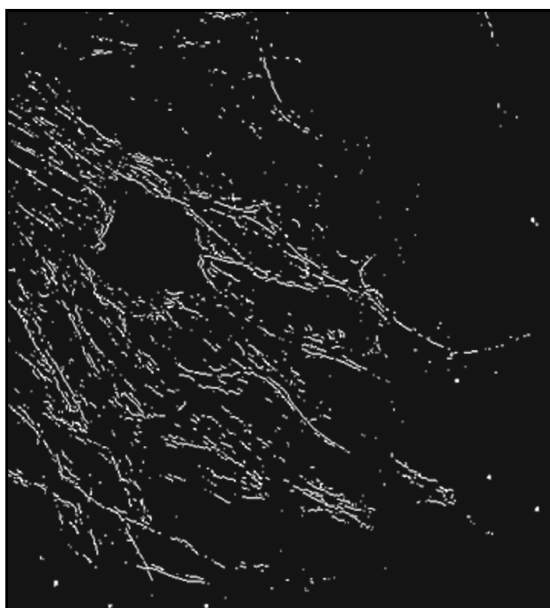


Fig.2: Image after Sobel Operation

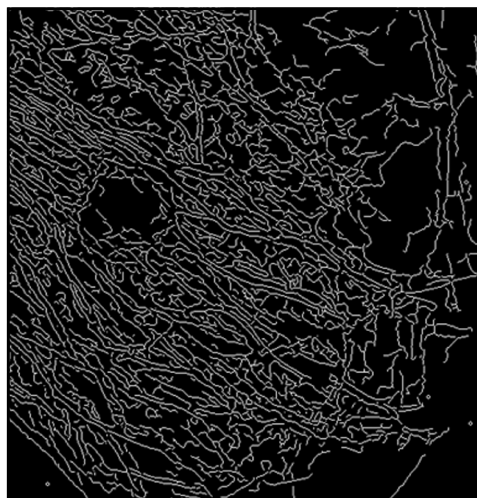


Fig. 3: Image after Canny Operation

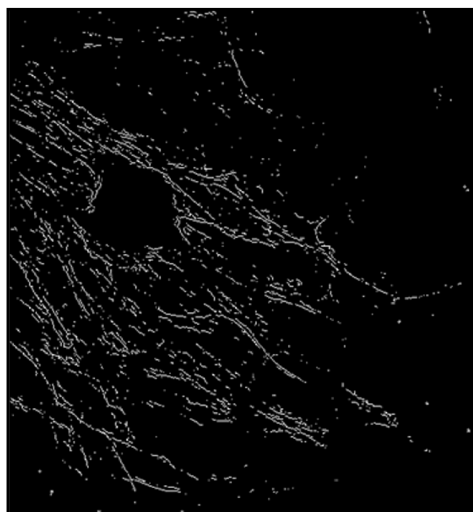


Fig. 4: Image after Robert Operation

Results of Proposed Method

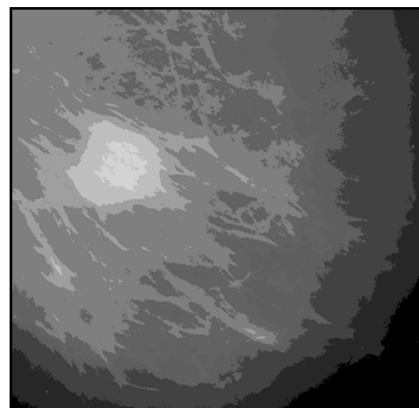


Fig.5: Output of Gaussian Low Pass Filter with Variance =2.5

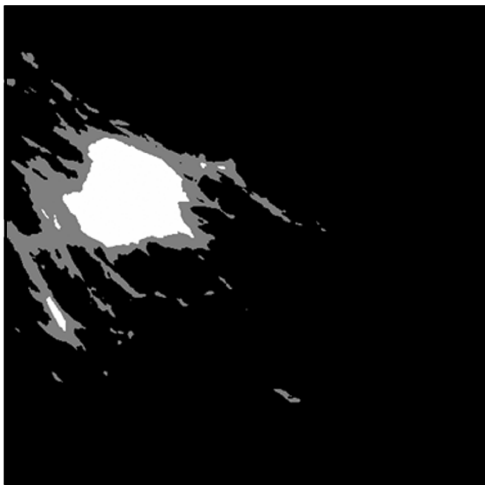


Fig.6: Image after NN Classifier

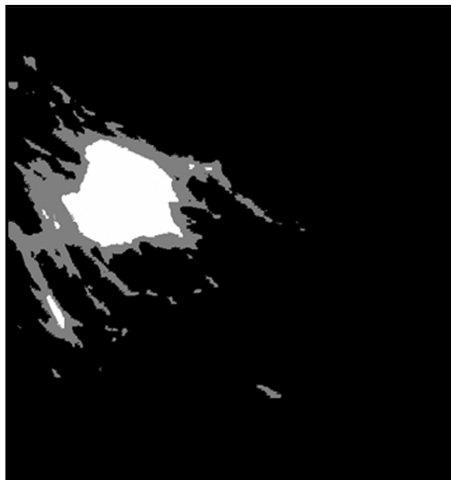


Fig.7: Image after N-ary Morphological Operator

5. CONCLUSION & FUTURE WORK

The proposed method removes the boundary errors successfully using combination of NN classifier and N-ary morphological operator. But, if the number of classes in the image is increases then difficult in designing the classifier and instead of Gaussian LPF, we can use Gabor filter for better noise removal and classification.

REFERENCES

- [1] A. K. Jain, F. Farrokhnia, "Unsupervised Texture Segmentation using Gabor Filters," *Pattern Recognition*, pp. 1167-1186, 1991.
- [2] M. Unser, "Texture Classification and Segmentation Using Wavelet Frames," *IEEE Trans. Image Proc.*, Pp. 1549-1560, 1995.
- [3] C.S. Lu, P.C. Chung, C.F. Chen, "Unsupervised Texture Segmentation Via Wavelet Transform," *Pattern Rec.*, Pp. 729-742, 1992.
- [4] T. P. Weldon and W. E. Higgins, "Designing Multiple Gabor Filters for Multi-Texture Image Segmentation," *Optical Engineering*, 38, No. 9 , Pp. 1478-1489 , Sept. 1999.
- [5] T. P. Weldon, W. E. Higgins, and D. F. Dunn, "Efficient Gabor Filter Design for Texture Segmentation," *Pattern Recognition* , 29, No. 12, pp. 2005-2015, Dec. 1996.
- [6] T. P. Weldon, W. E. Higgins, and D. F. Dunn, "Gabor Filter Design for Multiple Texture Segmentation," *Optical Engineering*, 35, No. 10, pp. 2852-2863, October 1996.
- [7] T. P. Weldon, "Improved Image Segmentation with a Modified Bayesian Classifier," *IEEE Transactions on Acoustics, Speech, and Signal Processing*, May 2006.
- [8] Anil K. Jain, *Fundamentals of Digital Image Processing*, Englewood Cliffs, NJ, Prentice Hall, 1989.
- [9] Raphael C. Gonzalez and Richard E. Woods, *Digital Image Processing*, Upper Saddle River, NJ, Prentice Hall, 2002.
- [10] R.N. Strickland and H.I. Hahn, "Wavelet Transform for Detecting Micro calcification in Mammograms", *IEEE Transaction on Medical Imaging*, 15, No.2, Pp.218-229, April 1996.
- [11] H. Yoshida, K. Doi, R.M. Nishikawa, "Automated Detection of Clustered Micro Calcification in Digital Mammograms using Wavelet Transform Techniques", *Proc. SPIE*, 21 67:868-886, 1994.
- [12] M.N. Gurcan, Y. Yardimci, A.E. Cetin and R. Ansari, "Automated Detection and Enhancement of Microcalcification on Digital Mammograms using Wavelet Transform Techniques", *Dept. of Radiology, Univ. of Chicago*, 1997.
- [13] S. Mallat, "A Theory for Multiresolution Signal Decomposition : The Wavelet Representation", *IEEE Trans. Pattern. Anal. Machine Intell.*
- [14] I. Daubechies, "Orthonormal Bases of Compactly Supported Wavelet", *Comm. on Pure and Applied Mathematics*, 41, pp.